the GB that were not considered in the theoretical studies. The presence of oxygen vacancies would remove negative charge from the area between the close Ti atom columns and thus increase the Ti-Ti distance, as found in our experiment.

We have shown how HRTEM can be used for direct imaging of the oxygen sublattice near a crystal defect in $SrTiO_3$ at atomic resolution. In addition to this structural information, a quantitative comparison with simulated HRTEM images should enable determination of the local chemical composition of oxides on the atomic scale. Our results strongly indicate that it should also be possible to resolve light elements in nonoxide materials such as borides, nitrides, or carbides. This would be of central importance for the understanding of defects in these materials.

References and Notes

1. I. Denk, J. Claus, J. Maier, *J. Electrochem. Soc.* **144**, 3526 (1997).
2. R. Waser, R. Hagenbeck, *Acta Mater.* **48**, 797 (2000).
3. Z. L. Zhang, W. Sigle, M. Rühle, *Phys. Rev. B* **66**, 094108 (2002).
4. Z. L. Zhang, W. Sigle, W. Kurtz, in preparation.
5. D. Brunner, S. Taeri-Baghbadrani, W. Sigle, M. Rühle, *J. Am. Ceram. Soc.* **84**, 1161 (2001).
6. C. Kisielowski *et al.*, *Ultramicroscopy* **89**, 243 (2001).
7. C. L. Jia, M. Lentzen, K. Urban, *Science* **299**, 870 (2003).
8. G. Möbus, F. Phillipp, T. Gemming, R. Schweinfest, M. Rühle, *J. Electron Microsc.* **46**, 381 (1997).
9. W. Kurtz, *Z. Metallkd.* **93**, 432 (2002).
10. P. A. Stadelmann, *Ultramicroscopy* **21**, 131 (1987).
11. The experimental image presented here was obtained from digital charge-coupled device camera recordings of the original negative films. It can grab image pixels from an area of 1536 × 1024 pixels at a spatial sampling rate of 0.013 nm/pixel. The displacement analysis was done in the negative image with DigitalMicrograph 3.6 (Gatan).
12. For δ_i^T and δ_i^S we only measured the spacing in the upper crystal because the contrast is more homogeneous in this part of the image. For δ_i^C we measured spacings from both the upper and lower crystals. The error bars correspond to the standard deviation determined from the statistical average.
13. S. Hutt, S. Köstlmeier, C. Elsässer, *J. Phys. Condens. Matter* **13**, 3949 (2001).
14. O. Kienzle, M. Exner, F. Ernst, *Phys. Status Solidi A* **166**, 57 (1998).

15. We thank U. Salzberger for excellent TEM specimen preparation, R. Höschen for his help during the operation of the ARM1250, and C. T. Koch and G. Richter for helpful discussions with the image simulations.

29 July 2003; accepted 25 September 2003

Is the Fragility of a Liquid Embedded in the Properties of Its Glass?

Tullio Scopigno,[1]* Giancarlo Ruocco,[1] Francesco Sette,[2] Giulio Monaco[2]

When a liquid is cooled below its melting temperature, it usually crystallizes. However, if the quenching rate is fast enough, the system may remain in a disordered state, progressively losing its fluidity upon further cooling. When the time needed for the rearrangement of the local atomic structure reaches approximately 100 seconds, the system becomes "solid" for any practical purpose, and this defines the glass transition temperature T_g. Approaching this transition from the liquid side, different systems show qualitatively different temperature dependencies of the viscosity, and accordingly they have been classified by introducing the concept of "fragility." We report experimental observations that relate the microscopic properties of the glassy phase to the fragility. We find that the vibrational properties of the glass well below T_g are correlated with the fragility value. Consequently, we extend the fragility concept to the glassy state and indicate how to determine the fragility uniquely from glass properties well below T_g.

When a liquid is cooled, the loss of kinetic energy leads to an ordering of the molecules, which then crystallize at the melting temperature T_m. However, if cooled fast enough through T_m, some materials (glass-forming materials) are capable of sustaining a metastable liquid state and, upon further cooling, of freezing into a disordered glassy state (*1*–*4*). The law that describes the change of the viscosity with the temperature approaching the glass transition temperature, T_g, is highly material-specific and has led to the classification of glass-forming materials according to the concept of "fragility" (*5*, *6*). The kinetic fragility, m, is directly related to the slowing down of the dynamics: It is defined in terms of the shear viscosity η as

$$m = \lim_{T \to T_g} \frac{d\log(\eta)}{d(T_g/T)}$$

Therefore, m is an index of how fast the viscosity increases while approaching the structural arrest at T_g, the temperature at which the structural relaxation time $\tau_\alpha \sim 100$ s. At this latter temperature, through the Maxwell relation $\eta = G_\infty \tau$, one finds a viscosity of $\eta \sim 10^{13}$ poise (more likely, $\eta \sim 10^{11}$ poise for molecular glasses), whereas 10^{-4} poise is the "infinite" temperature limit in basically any material. Consequently, fragility values typically range between $m = 17$ for "strong" systems (those that show an Arrhenius behavior) and $m \sim 150$ for "fragile" systems, where the high cooperativity of the diffusive dynamics induces a high (and T-dependent) apparent activation energy. One interesting element of this classification lies in the attempt to relate the temperature behavior of a macroscopic transport property close to T_g to the microscopic interactions driving the dynamics of the system. It has been found, for example, that the value of the fragility is empirically related to the kind of interaction potential among the particles constituting the system. Prototypical examples of fragile liquids are those composed by units interacting via isotropic bonds, such as van der Waals–like molecular liquids. The strong glass-forming liquids, on the other hand, are those characterized by strong covalent directional bonds that form space-filling networks. *O*-terphenyl ($m = 80$) and SiO_2 ($m = 20$) are characteristic examples of a fragile and a strong liquid, respectively. Hydrogen-bonded systems, such as glycerol ($m = 50$), are often called "intermediate" between strong and fragile liquids. Kinetic fragility has been found to be correlated to other properties of the glass-forming liquids, such as (i) the slope at T_g of the temperature dependence of the configurational entropy (often referred to as thermodynamic fragility) (*7*) or (for classes of systems sharing similar T_g's) the specific heat jump at T_g (*8*, *9*); (ii) the ratio between the maximum and the minimum of the boson peak; that is, of the bump observed at terahertz frequencies in the Raman and neutron-scattering spectra of glass-forming materials (*10*) [although this finding is controversial (*11*)]; (iii) the degree of stretching in the nonexponential decay of the correlation functions in the liquid close to T_g (*12*); (iv) the statistics of the minima in a potential energy landscape–based description (*13*, *14*) of the diffusion process in supercooled liquids (*15*–*17*); and, more recently, (v) the temperature behavior of the shear elastic modulus in the supercooled liquid (*18*). In all these studies, the fragility has been always related to (or defined through) macroscopic properties characterizing the liquid side of the glass transition. Although there are attempts to relate the fragility to the anharmonicity of the "hot" glass (*19*), no connection has been found up to now between the

[1]Istituto Nazionale per la Fisica della Materia and Dipartimento di Fisica, Universitá di Roma La Sapienza, 00185 Roma, Italy. [2]European Synchrotron Radiation Facility, BP 220, 38043 Grenoble, France.

*To whom correspondence should be addressed. E-mail: tullio.scopigno@phys.uniroma1.it

value of m and the physical properties of the low-temperature glassy phase.

We show that, starting from a determination of the nonergodicity factor in the low-temperature glass, it is possible to identify a parameter that controls how fast the nonergodicity factor decreases when the temperature is increased, and that turns out to be proportional to the fragility m. Through this, we establish a way to determine the fragility of a system in the glassy phase well below T_g, independent of the way in which viscosity changes with decreasing temperature from the liquid side. By exploiting the harmonic approximation of the low-temperature dynamics, it is found that this parameter only depends on the characteristics of the static disorder, which in turn controls the vibrational eigenmodes of the glass. This result demonstrates the existence of a deep link between the diffusive interbasin dynamics and the vibrational intrabasin dynamics in glass-forming systems.

Recent extensive inelastic x-ray scattering (IXS) measurements of the dynamic structure factor have allowed a sizeable library of high-frequency (terahertz) dynamical properties of glasses to be constituted. Of interest here is the fact that the IXS measurements allow for the determination of the nonergodicity factor $f(Q,T)$, with a reliability that was not achievable via light or neutron scattering (*20*). The nonergodicity factor is the long time limit of the density correlator $\Phi_Q(t)$; that is, the density-density correlation function $F(Q,t)$, normalized to the static structure factor $S(Q)$: $\Phi_Q(t) = F(Q,t)/S(Q)$. The quantity $1 - f(Q,T)$ represents the amount of decorrelation introduced by the vibrational dynamics, and it depends on both the (T-dependent) amplitude of the vibrations and the degree of disorder of the glassy structure. In a low-temperature glass, $F(Q,t)$, apart from the Debye-Waller factor $\exp[-W(Q)]$, can be expressed as the sum of a constant term $S_{IS}(Q)$, which represents the static structure factor of the atomic equilibrium positions (inherent structure), plus a time-dependent one, $F_{inel}(Q,t)$, which is the contribution of the atomic vibration around such equilibrium positions, a quantity that vanishes in the long time limit

$$F(Q,T) = e^{-W(Q)}[S_{IS}(Q) + F_{inel}(Q,t)] \quad (1)$$

Therefore,

$$f(Q,T) = \lim_{t\to\infty} \Phi_Q(t) = \lim_{t\to\infty} \frac{S_{IS}(Q)+F_{inel}(Q,t)}{S_{IS}(Q)+S_{inel}(Q)} = \frac{1}{1+S_{inel}(Q)/S_{IS}(Q)} \quad (2)$$

where we have defined $S_{inel}(Q) \doteq F_{inel}(Q,t=0)$. $S(Q,\omega)$ is the Fourier transform of $F(Q,t)$ and is the quantity directly accessible in scattering experiments. From Eq. 1 it can be expressed as

$$S(Q,\omega) = e^{-W(Q)}[S_{IS}(Q)\delta(\omega) + S_{inel}(Q,\omega)] \quad (3)$$

From an experimental point of view and according to Eqs. 2 and 3, the nonergodicity factor is derived from the ratio of the elastic to the inelastic scattered intensity, obtained from inelastic scattering measurements of the dynamic structure factor $S(Q,\omega)$ (*21*). A sense of the T dependence of $f(Q,T)$ can be obtained from Fig. 1. Here, as an example, we report the IXS spectra at fixed exchanged wave vector ($Q = 2$ nm^{-1}) and at different temperatures in glycerol. The inelastic (dashed lines) and elastic (dotted

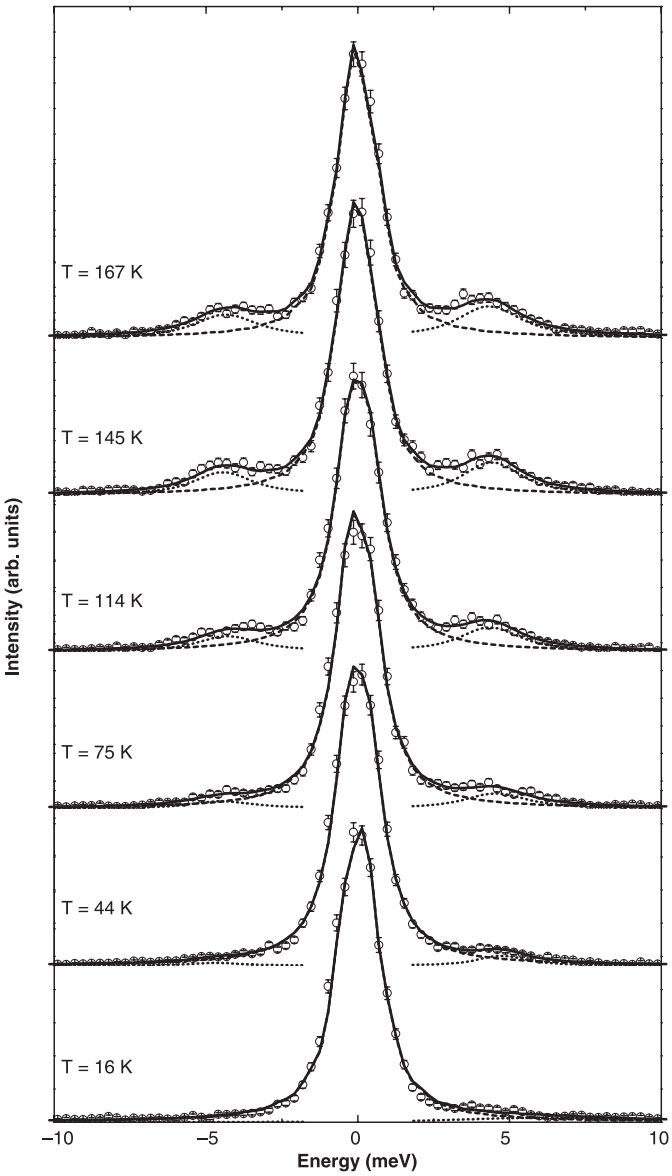

Fig. 1. Selected example of the inalastic x-ray scattering energy spectra of glycerol (open circles with error bars) taken at $Q = 2$ nm^{-1} at the indicated temperatures. The solid line is the line of best fit according to Eq. 3 and eq. S2, whereas the dashed and dotted lines are the elastic and inelastic contributions, respectively (see the supporting online material for further details). The values of $f(Q,T)$ are obtained by the ratio of the integrated intensities of the elastic and inelastic contribution, from Eq. 2. arb., arbitrary.

Table 1. Temperature steepness of the viscosity at T_g (fragility) and of the nonergodicity factor at $T \to 0$ (α) for several materials.

Sample	T_g (K)	m	α
BeF_2*	598	20	0.16
Silica†	1450	28	0.19
Glycerol‡	190	53	0.32
$PB_{1.4}$§	180	60	0.40
nBB‖	125	53	0.46
Salol¶	218	73	0.64
mtol#	187	77	0.57
oTP**	241	81	0.58
mTCP††	205	87	0.59
Se‡‡	308	87	0.7

*m from (*26*), α from (*27*). †Silica infrasil-grade sample. m from (*12*), α from (*28*) and references therein. ‡m from (*12*), α from (*29*). §Polybutadiene: α is determined from an experiment performed on a sample constituted of 1.4 structural units only, reported in (*30*). The fragility is not directly available for such a composition; we estimated m by extrapolating data for several concentrations of mixtures composed of 1.2 and 1.4 structural units, available from (*12*, *31*). ‖Normal butyl-benzene: m from (*32*), α from the experiment in (*33*). ¶m from (*12*), α from unpublished data. #Metatoluidine: m from (*34*), α from unpublished data. **O-terphenyl: m from (*12*), α from (*35*). ††Metatricresylphosphate: m from (*12*), α from unpublished data. ‡‡m from (*12*), α from unpublished data.

lines) contributions to the scattering intensity are shown, and one can appreciate in the raw data the change of relative intensity as a function of T. As far as the Q dependence is concerned, $f(Q,T)$ follows in phase the oscillations of the static structure factor and is almost Q-independent in the $Q \rightarrow 0$ region, where $S(Q)$ is almost constant (*22*), (see the inset of Fig. 2). We focus on this small-Q region. From the integrated intensities of the elastic and inelastic contributions, obtained by a fitting procedure (see eqs. S1 and S2 of the supporting on line material), the T dependence of $f(Q,T)$ is obtained. The values of $f(Q,T)^{-1}$ (which is expected to be linear in T) are reported in Fig. 2 (triangles). Also reported in the same figure is the T dependence of $f(Q,T)$ for two other archetypical glasses: silica and *O*-terphenyl (oTP).

To better understand the temperature dependence of $f(Q,T)$ in the $T \rightarrow 0$ limit, we invoke the harmonic approximation for the vibrational dynamics. This allows one to express $f(Q,T)$ in terms of the vibrational properties of the systems; that is , the eigenvalues (ω_p) and eigenvectors ($\bar{e}_p$) of the potential energy Hessian, evaluated at the inherent structure. Using the harmonic approximation for $S_{inel}(Q,\omega)$, it is straightforward (*23*, *24*) to show that Eq. 2 reduces to

$$f(Q,T) = \left[1 + \frac{K_B T Q^2}{M S_{IS}(Q)} \frac{1}{N} \sum_p \frac{\left| \Sigma_i [\hat{Q} \cdot \bar{e}_p(i)] e^{iQr_i} \right|^2}{\omega_p^2} \right]^{-1} \quad (4)$$

Here M is the molecular mass, K_B is the Boltzmann constant, and i is summed over the N particles and p over the $3N$ normal modes. In order to pinpoint the T dependence of the nonergodicity factor in the low Q limit, it is convenient to rewrite Eq. 4 as

$$f(Q \rightarrow 0, T) = \frac{1}{1 + \alpha \frac{T}{T_g}} \quad (5)$$

We thus define the dimensionless quantity α, which encompasses all the microscopic details of the system, as the eigenvalues and eigenvectors of the normal modes. These are quantities that, in turn, depend on the interaction potential and on the disordered structure. This equation provides a formal way to extract the system-dependent parameter α from the T dependence of $f(Q,T)$, derived from the IXS data. This has motivated us to revisit the large amount of IXS data available for glasses at low T, where the harmonic approximation, and therefore Eq. 5, is expected to be valid. As it can be seen in Fig. 2, the observed T dependence of $f(Q,T)$ is fully consistent with the functional form predicted by Eq. 5, and this allows us to determine α by a least-squares minimization procedure. The derived values for α (such as $\alpha = 0.19$ for silica, $\alpha = 0.32$ for glycerol, and $\alpha = 0.58$ for oTP) clearly indicate a trend: The more fragile a liquid, the greater the slope of $f(Q,T)$ at $T = 0$; that is, the faster the decorrelation of the density fluctuations on increasing T. The fitting procedure has been applied to the whole set of available glasses, and the obtained values of α are reported in Table 1 and Fig. 3 as a function of the independently known fragility parameter m. Figure 3 clearly shows the existence of a strong correlation between m and α: The higher the fragility, the higher the value of α; that is, the faster is the T dependence of the $f(Q,T)$ parameter. The existence of a strong correlation between α and m is further emphasized by the empirical observation that the two quantities are not only correlated but (within the statistical accuracy) are actually proportional to each other, according to the relation $m = (135 \pm 10)\alpha$. In passing, we note that the two points that lie definitely below the dotted line (selenium and salol) are the ones for which fragility determined at T_g doesn't agree well with the fragilities determined at higher temperatures (*7*, *25*).

The observed correlation is conceptually surprising. It indicates the existence of a link between the curvatures of the potential energy function at its minima (more specifically, those visited in the glassy phase) and the other properties of the potential energy function (the energy distribution of the minima, minimum-to-minimum barrier height, distribution of the saddle order and energies, etc.) controlling the diffusive processes in supercooled liquids.

We further examine how α emerges from the collective density-density correlation function plateau. From Eqs. 4 and 5, the microscopic expression for α is found to be

$$\alpha = \left[\frac{K_B T_g Q^2}{M S_{IS}(Q)} \frac{1}{N} \sum_p \frac{\left| \Sigma_i [\hat{Q} \cdot \bar{e}_p(i)] e^{iQr_i} \right|^2}{\omega_p^2} \right]^{-1} \quad (6)$$

One may in principle derive a similar parameter α_s from the temperature dependence of the self-correlator plateau. In this case, α_s is related to the familiar mean square displacement.

The harmonic approximation for theDebye-Waller factor $f_s(Q,T) = \exp[-W(Q,T)]$ would lead to an equation formally identical to Eq. 5, but with α replaced by α_s

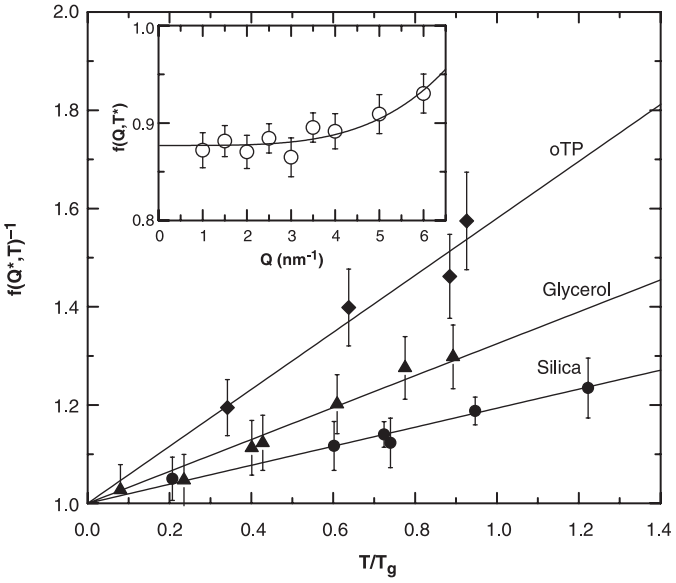

Fig. 2. Values of $f(Q^*,T)^{-1}$ (Eq. 2) for $Q^* \cong 2$ nm^{-1} reported in a T/T_g scale for three representative materials (solid symbols with error bars): silica (T_g = 1450 K), glycerol (T_g = 190 K), and oTP (T_g = 241 K). The full line is the best fit of the experimental data to Eq. 5. These fits have been used to derive the values of α reported in Fig. 3. The inset shows the Q dependence of $f(Q,T^*)$ for silica at T^* = 1050 K.

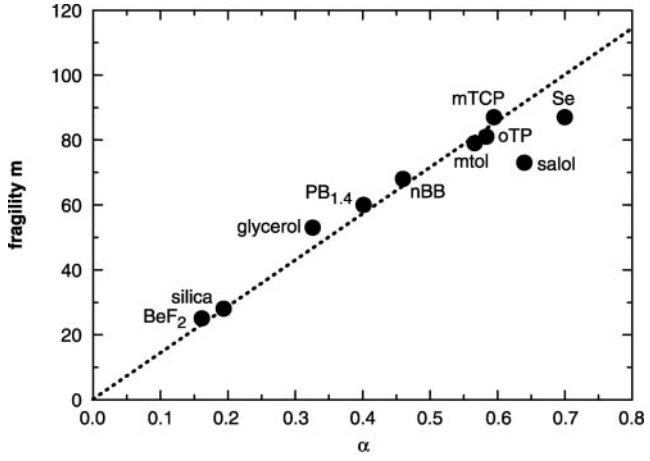

Fig. 3. Correlation plot of the kinetic fragility and the α parameter of the nonergodicity factor (Eq. 5). The dotted line is obtained by a fit of the data to a linear equation. It corresponds to $m = 135\alpha$, and the regression coefficient is $r = 0.994$.

$$\alpha_s = \left[\frac{K_B T_g Q^2}{M} \frac{1}{N} \sum_p \frac{1}{\omega_p^2} \right]^{-1} \quad (7)$$

Therefore α and α_s differently weight the low-frequency modes. Specifically, in the small Q limit, α is more sensitive to the low-energy modes than α_s, which, independently of Q, reflects the whole density of states. It would be interesting to investigate whether these two quantities are correlated with each other.

Here we report evidence for correlation between the fragility of a glass-forming liquid and the temperature dependence of its nonergodicity factor, as determined by the vibrational dynamics at very low temperatures. The fragility is an index of how the viscosity increases upon supercooling. The nonergodicity factor, in the low temperature limit, is related to the vibrational properties of the harmonic glassy dynamics (Eq. 6); that is, to the curvature of the energy minima. Therefore, from our finding it emerges that the properties of the potential energy landscape around the deep minima are related to those properties that control the diffusion of the system through different basins. This unexpected relation is a further aspect of the physics of the glass transition that needs to be clarified.

References and Notes

1. K. Ngai, Ed., *J. Non-Cryst. Solids* **307–319** (special issue) (2002).
2. M. Giordano, D. Leporini, M. Tosi, Eds., *J. Phys. Condens. Matter* **11** (special issue) (1999).
3. L. Andreozzi, M. Giordano, D. Leporini, M. Tosi, Eds., *J. Phys. Condens. Matter* **15** (special issue) (2003).
4. P. G. Debenedetti, F. H. Stillinger, *Nature* **410**, 259 (2001).
5. C. A. Angell, *J. Non-Cryst. Solids* **131-133**, 13 (1991).
6. C. A. Angell, *Science* **267**, 1924 (1995).
7. L.-M. Martinez, C. A. Angell, *Nature* **410**, 663 (2001).
8. D. Huang, G. McKenna, *J. Chem. Phys.* **13**, 5621 (2001).
9. K. Ngai, O. Yamamuro, *J. Chem. Phys.* **23**, 10403 (1999).
10. A. Sokolov, E. Rössler, A. Kisliuk, D. Quittman, *Phys. Rev. Lett.* **71**, 2062 (1993).
11. S. Yannopoulos, G. Papatheodorou, *Phys. Rev. E* **62**, 3728 (2000).
12. R. Böhmer, K. L. Ngai, C. A. Angell, D. J. Plazek, *J. Chem. Phys.* **99**, 4201 (1993).
13. M. Goldstein, *J. Chem. Phys.* **51**, 3728 (1969).
14. W. H. Stillinger, T. A. Weber, *Phys. Rev. A* **25**, 978 (1982).
15. R. Hall, P. Wolynes, *J. Chem. Phys.* **86**, 2943 (1987).
16. R. J. Speedy, *J. Phys. Chem. B* **103**, 4060 (1999).
17. S. Sastry, *Nature* **409**, 164 (2001).
18. J. C. Dyre, N. Olsen, preprint available at http://xxx.lanl.gov/abs/cond-mat/0211042.
19. C. A. Angell, in *Proceedings of the International School of Physics Enrico Fermi, Course CXXXIV*, F. Mallamace, H. E. Stanley, Eds. (IOS Press Amsterdam, Netherlands, 1997), vol. 11.
20. F. Sette, M. Krisch, C. Masciovecchio, G. Ruocco, G. Monaco, *Science* **280**, 1550 (1998).
21. Some fraction of the elastic line may in principle be related to the nonpropagating temperature fluctuations. The amount of this contribution is actually ruled out by the quantity $[(c_p)/(c_v)] - 1 = \gamma - 1$, and therefore it vanishes in the $T \rightarrow 0$ limit when $\gamma \rightarrow 1$ holds according to the harmonic approximation.
22. A. Tölle, H. Schober, J. Wuttke, F. Fujara, *Phys. Rev. E* **56**, 809 (1997).
23. G. Ruocco, *et al.*, *Phys. Rev. Lett.* **84**, 5788 (2000).
24. T. Scopigno, G. Ruocco, F. Sette, G. Viliani, *Phys. Rev. E* **66**, 031205 (2002).
25. J. Garrahan, D. Chandler, *Proc. Natl. Acad. Sci. U.S.A.* **100**, 9710 (2003).
26. M. Hemmati, C. T. Moynihan, C. A. Angell, *J. Chem. Phys.* **115**, 6663 (2001).
27. T. Scopigno *et al.*, *J. Chem. Phys.* **118**, 311 (2003).
28. C. Masciovecchio *et al.*, *Phys. Mag. B* **79**, 2013 (1999).
29. G. Ruocco *et al.*, *Phys. Rev. Lett.* **83**, 5583 (1999).
30. D. Fioretto *et al.*, *Phys. Rev. E* **59**, 4470 (1999).
31. R. Zorn, G. B. McKenna, L. Willner, D. Richter, *Macromolecules* **28**, 8552 (1995).
32. C. Hansen, F. Stickel, R. Richert, E. W. Fisher, *J. Chem. Phys.* **108**, 6408 (1998).
33. C. Masciovecchio *et al.*, *Phys. Rev. Lett.* **80**, 544 (1998).
34. B. M. Erwin, R. H. Colby, *J. Non-Cryst. Solids* **307-310**, 225 (2002).
35. G. Monaco, C. Masciovecchio, G. Ruocco, F. Sette, *Phys. Rev. Lett.* **80**, 2161 (1998).

36. The authors gratefully acknowledge C. A. Angell for valuable hints and suggestions and J. Dyre, S. Sastry, F. Sciortino, and S. Yannopoulos for fruitful discussions.

Supporting Online Material

www.sciencemag.org/cgi/content/full/302/5646/849/DC1
Methods
References

21 July 2003; accepted 24 September 2003

Decadal Variation of the Surface Water PCO_2 in the Western and Central Equatorial Pacific

Taro Takahashi,[1]* Stewart C. Sutherland,[1] Richard A. Feely,[2] Catherine E. Cosca[2]

The equatorial Pacific Ocean is one of the most important yet highly variable oceanic source areas for atmospheric carbon dioxide (CO_2). Here, we used the partial pressure of CO_2 (PCO_2), measured in surface waters from 1979 through early 2001, to examine the effect on the equatorial Pacific CO_2 chemistry of the Pacific Decadal Oscillation phase shift, which occurred around 1988 to 1992. During the decade before the shift, the surface water PCO_2 (corrected for temperature changes and atmospheric CO_2 uptake) in the central and western equatorial Pacific decreased at a mean rate of about –20 μatm per decade, whereas after the shift, it increased at about +15 μatm per decade. These changes altered the CO_2 sink and source flux of the equatorial Pacific significantly.

The equatorial Pacific Ocean is known to undergo significant changes on interannual time scales (e.g., El Niño and La Niña) and on decadal time scales. This area is a major source of CO_2 to the atmosphere during non–El Niño periods (*1–5*) but near neutral during strong El Niño periods (*2–5*). Over decadal time scales, the North Pacific Ocean has undergone major physical and biological changes commonly called the Pacific Decadal Oscillation (PDO) (*6–9*). The most recent and major shifts of 1977 and 1988 to 1992 have been documented on the basis of extensive physical and biological information (*6–8*). Although the causes and effects of PDO have been investigated in recent years, its effects on CO_2 chemistry have not yet been identified. Here, we describe the changes in CO_2 chemistry in the Pacific equatorial waters associated with the 1988 to 1992 PDO phase shift (*6–8*) using the partial pressure of CO_2 (PCO_2) in seawater, which is a measure of the escaping tendency of CO_2 from seawater to the overlying atmosphere.

Because of the heightened interest in the El Niño–Southern Oscillation (ENSO) events and the carbon cycle, PCO_2 in surface ocean waters has been measured more frequently since 1979 over the equatorial Pacific Ocean. In this study, we assembled a database containing about 100,000 PCO_2 observations made in surface waters of the equatorial belt, 5°N to 5°S, between April 1979 and March 2001 (*10*). We classified these into three groups: (i) the Niño 3.4 area (lat 5°S to 5°N, long 170°W to 120°W) during non–El Niño periods (which include La Niña periods); (ii) the Niño 3.4 area during El Niño periods; and (iii) the western warm pool area (lat 5°N to 5°S, long 175°E to 135°E). We identified six El Niño periods in the Niño 3.4 area on the basis of sea surface temperature (SST) anomalies (*11*). The remaining data were considered as occurring during non–El Niño periods.

In the Niño 3.4 area, observations during non–El Niño periods were made more or less evenly throughout the year along a total of 11 meridional transects across the equator during the pre-1990 period, and 14 transects during the post-1990 period. In this area, no measurements

[1]Lamont-Doherty Earth Observatory (LDEO) of Columbia University, Palisades, NY 10964, USA. [2]Pacific Marine Environmental Laboratory (PMEL), National Oceanic and Atmospheric Administration (NOAA), Seattle, WA 98115, USA.

*To whom correspondence should be addressed. E-mail: taka@ldeo.columbia.edu